TMR

ARTICLE

TMR Modern Herbal Medicine 2022;5(4):24. https://doi.org/10.53388/MHM2022A1104001

New flavanone-monoterpene hybrids as α-glucosidase inhibitors from the root bark of *Morus alba*

Lin-Lin Tian[1], Hua Zhang[1,*]

[1] School of Biological Science and Technology, University of Jinan, Jinan 250022, China.

***Corresponding to** Hua Zhang. School of Biological Science and Technology, University of Jinan, No. 336, West Road of Nan Xinzhuang, Shizhong District, Jinan 250022, China. E-mail: bio_zhangh@ujn.edu.cn

Author contributions

Lin-Lin Tian performed the experimental work, data collection and analyses, and prepared the draft manuscript. Hua Zhang supervised the project, analyzed the data and edited/revised the manuscript.

Competing interests

The authors declare no conflict of interests.

Acknowledgments

Financial support is from the Natural Science Foundation of Shandong Province for Distinguished Young Scholars (No. JQ201721).

Abbreviations

HPLC, High performance liquid chromatography; NMR, Nuclear magnetic resonance; ECD, Electronic circular dichroism; UV, Ultraviolet; HR-ESIMS, High resolution electrospray ionization mass spectroscopy; Q-TOF, Quadrupole-time-of-flight; RP-C_{18}, Reversed-phase C_{18}; CC, Column chromatography; TLC, Thin-layer chromatography; DMSO, Dimethyl sulfoxide; PNPG, 4-nitrophenyl-β-D-glucopyranoside; OD, Optical density; IC_{50}, Half maximal inhibitory concentration; r.t., room temperature.

Peer review information

TMR Modern Herbal Medicine thanks all anonymous reviewers for their contribution to the peer review of this paper.

Citation

Tian LL, Zhang H. New flavanone-monoterpene hybrids as α-glucosidase inhibitors from the root bark of *Morus alba*. *TMR Modern Herb Med*. 2022;5(4):24. doi: 10.53388/MHM2022A1104001.

Executive editor: Chao-Yong Wu.
Received: 4 November 2022;
Accepted: 25 November 2022;
Available online: 30 November 2022.

Abstract

Objective The *Morus alba* root bark is a well-known Chinese herbal medicine called Sang-Bai-Pi and has often been used to relieve the hyperglycemic symptom of diabetes patients. The current work aims to further explore its bioactive constituents with α-glucosidase inhibitory activity for the potential treatment of diabetes.

Methods A combination of different separating techniques including routine column chromatograph and HPLC especially on chiral columns were applied for the isolation of target molecules, while comprehensive spectroscopic experiments comprising MS, NMR, ECD, etc. were carried out to complete the structural assignment. The anti-hyperglycemic property of the isolates was evaluated by an *in vitro* α-glucosidase inhibitory bioassay.

Results Two pairs of new flavanone-monoterpene hybrid enantiomers were isolated and identified, and an interesting phenomenon of mutual transformation between these cometabolites were detected, which resulted in their regio-isomerization and enantiomerization. The bioassay results revealed remarkable α-glucosidase inhibitory activity for these fascinating molecules.

Conclusions The *Morus alba* root bark is a rich source of bioactive flavonoid derivatives and deserves further investigations to develop new potential chemotherapies for diabetes control and treatment.

Keywords *Morus alba;* Flavanone, Regio-isomerization; Enantiomerization; α-Glucosidase inhibition

Root barks of *Morus alba*

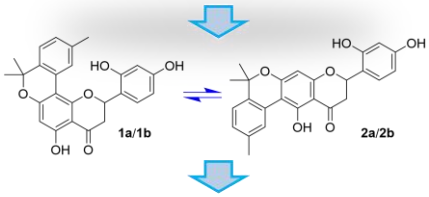

α-glucosidase inhibition

Compds.	IC_{50}(μM)
1a/1b	4.05 ± 0.65
2a	3.06 ± 0.42
2b	6.69 ± 0.51

Highlights

1. Two pairs of new flavanone-monoterpene hybrid enantiomers were separated and structurally characterized from *Morus alba* root bark;
2. An interesting transformation between these cometabolites leading to regio-isomerization and enantiomerization was observed;
3. The equilibrium mixtures showed significant inhibition against the diabetes target α-glucosidase.

Introduction

Morus alba L. is likely the most famous plant species of family Moraceae owing to its tremendous economic values with both dietary and medicinal benefits [1]. Its fruits, also known as mulberry, have been serving as a food for thousands of years in China and its tender shoots have also been developed into a vegetable dish by local residents of Huzhou city. Meanwhile, the twigs and root barks of *M. alba* have been listed by the National Health Commission of China in a catalogue of medicinal species that can be added into functional foods. Therefore, the investigations on *M. alba* have always been a front-line topic in the scientific community as summarized in recent years' review articles [2–5].

The root barks of *M. alba* are a well-known species collected by the National Pharmacopeia of China as one of the commonly used herbal medicines, and they have been used to treat edema, cough, dyspnea, etc. in traditional Chinese medicine [6]. Although the study on the root barks of the title plant can be tracked back to a half-century ago [7], related phytochemical and pharmacological researches have still been very active in recent years. These investigations have revealed that the *M. alba* root barks represent a very rich source of bioactive phenolic compounds especially prenylated flavonoids and benzofuran derivatives that have shown a variety of biological activities comprising anti-diabetic [8, 9], anti-inflammatory [10–12], anti-tumor [13, 14], anti-neurodegenerative [15, 16], and antiviral properties [12, 17]. As a continuation of our previous work for anti-hyperglycemic agents from small molecule natural products in medicinal plants [18–20], we have recently carried out an intensive study on the bioactive constituents from the root barks of *M. alba*, leading to the discovery of two pairs of flavanone-monoterpene hybrid enantiomers (Figure 1). The isolation, structure identification and α-glucosidase inhibitory evaluation of these compounds will be presented here.

Materials and Methods

General instrumentation and reagents

$[\alpha]_D$ values were measured on a Rudolph VI polarimeter (Rudolph Research Analytical, Hackettstown, USA) using a 10 cm length cell. UV and ECD spectra were acquired on a Chirascan Spectrometer (Applied Photophysics Ltd., Leatherhead, UK). NMR experiments were performed on a Bruker Avance DRX600 spectrometer (Bruker BioSpin AG, Fällanden, Switzerland) and the residual peaks of deuterated solvents (methanol-d_4: δ_C 49.00 and δ_H 3.31 ppm; acetone-d_6: δ_C 29.84, 206.26 and δ_H 2.05) were used as internal references. HR-ESIMS spectra were recorded on an Agilent 6545 Q-TOF mass spectrometer (Agilent Technologies Inc., Waldbronn, Germany). D-101 macroporous resin (Sinopharm Chemical Reagent Co. Ltd., Shanghai, China), reversed-phase (RP) C_{18} (Merck KGaA, Darmstadt, Germany) and silica gel (300–400 mesh, Qingdao Marine Chemical Co. Ltd., Qingdao, China) were used for routine column chromatography (CC). Agilent SB-C_{18} column (5 μm, 9.4×250 mm, Agilent Technologies Inc., Santa Clara, USA) and Daicel AD-H chiral column (5 μm, 4.6×250 mm, Daicel Chiral Technologies Co. Ltd., Shanghai, China) were used for HPLC analyses and separations. Thin-layer chromatography (TLC) was conducted with pre-coated silica gel GF_{254} plates (Qingdao Marine Chemical Co. Ltd., Qingdao, China). Analytical and HPLC grade solvents were acquired from Tianjin Fuyu Fine Chemical Co. Ltd. (Tianjin, China) and Oceanpak Alexative Chemical Ltd. (Goteborg, Sweden), respectively.

Plant materials

The roots of *Morus alba* L. (family Moraceae) were collected in August 2016 in Mount Kunyu, Shandong province, China, and the plant materials were identified by Prof. Guo-hua Ye from Shandong College of Traditional Chinese Medicine. The voucher specimen has been deposited in the author's institution with an accession number npmc-025.

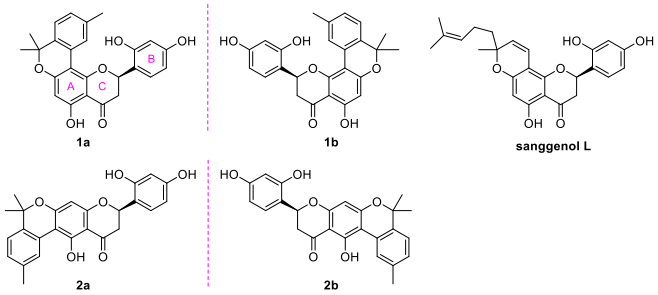

Figure 1. Chemical structures of compounds from the root bark of *Morus alba*.

Extraction and isolation

The barks of *M. alba* roots (30 kg) were peeled, dried and milled, and the powder was extracted with 95% EtOH (50 L) at r.t. for three times (once a week). The extracting solution was condensed under reduced pressure and the residue (3.6 kg) was re-suspended in 5.0 L water and partitioned with ethyl acetate (3.0 L × 3). The organic phase was solvent-removed (1.5 kg) and then fractionated by a macroporous resin CC with 30% (30 L), 50% (50 L), 80% (80 L) and 95% (50 L) EtOH-H_2O successively. Each eluting component was concentrated under reduced pressure on a large-scale rotary evaporator. The 80% EtOH-H_2O eluent (600 g) was separated by silica gel CC (petroleum ether-EtOAc, 20:1 to 1:2) to give 14 fractions A to N, and fraction K (4.0 g) was subsequently processed by a RP-C_{18} column (50%–100% MeOH-H_2O) to obtain eight further subfractions (K1 to K8). Subfraction K6 was eluted with CH_2Cl_2-MeOH (1000:1 to 100:1) on a silica gel column to afford seven new eluents (K6-1 to K6-7), and then the K6-6 eluent was purified by semi-preparative HPLC on an Agilent SB-C_{18} column eluted with 70% MeCN-H_2O (3.0 mL/min) to yield a mixture containing compounds **1a**/**1b** and **2a**/**2b** (2.3 mg, t_R = 18.0 min). This mixture was further fractionated by a Daicel AD-H column eluted with 12% isopropanol-*n*-hexane (1.0 mL/min) to give compounds **1a** (0.2 mg, t_R = 9.5 min), **1b** (0.4 mg, t_R = 10.5 min), **2a** (0.5 mg, t_R = 16.0 min) and **2b** (0.8 mg, t_R = 19.0 min).

Compounds **1a**/**1b** and **2a**/**2b**: Yellow amorphous powder; $[\alpha]^{27}_D$ ~0; UV (MeOH) λ_{max} (log ε) 277 (4.72) nm; ^{1}H and ^{13}C NMR data, see Table 1; (+)-ESIMS *m/z* 419.3 $[M + H]^+$; (+)-HR-ESIMS *m/z* 419.1487 $[M + H]^+$ (calcd for $C_{25}H_{22}O_6$, 419.1495).

α-Glucosidase inhibitory assay.

The *in vitro* inhibition against α-glucosidase of compounds **1a**/**1b**, **2a** and **2b** was screened according to the protocol documented previously [21]. The testing concentration of α-glucosidase was set as 0.4 U/mL. The inhibitory activity of the three samples was first tested at 100 μM, and all samples showing >50% inhibition ratio would be sent for further IC_{50} measurements. The positive control acarbose (Aladdin, Shanghai, China) showed an IC_{50} of 359.10 ± 2.39 μM in the present work.

Results and Discussion

Compounds **1a**/**1b** and **2a**/**2b** were first obtained via routine HPLC separation as yellow amorphous powder, with the molecular formula $C_{25}H_{22}O_6$ determined by HR-ESIMS analysis at *m/z* 419.1487 ($[M + H]^+$, calcd for 419.1495). The ^{1}H and ^{13}C NMR spectra of this sample in both CD_3OD and CD_3COCD_3 (Supplemental Figures S1, S2, S7 and S8) exhibited two sets of signals indicating the presence of two different molecules. However, subsequent fractionation of this mixture on several other normal HPLC columns did not gain further separation. A Daicel AD-H chiral column was then used to check for further separation, which unexpectedly revealed four peaks (**1a**, **1b**, **2a** and **2b**) in the HPLC chromatogram (Figure 2). The ^{1}H NMR spectra of the two major peaks (**2a** and **2b**) were then measured in CD_3OD and CD_3COCD_3, respectively, and the spectra were compared to those of the original mixture sample (Supplemental Figure S20), which demonstrated that both of them had identical ^{1}H NMR data with those of the major component, while those of the one (**1b**) from the two minor peaks were also measured in the two deuterium solvents and proved to be identical with those of the minor component in the mixture. These observations indicated that the two sets of signals in the initial NMR spectra corresponded to two pairs of enantiomers, namely **1a**/**1b** and **2a**/**2b** (Figure 2).

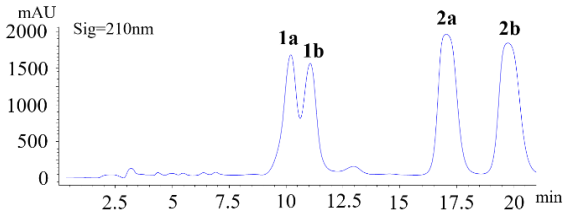

Figure 2. Chiral HPLC separation for 1a, 1b, 2a and 2b.

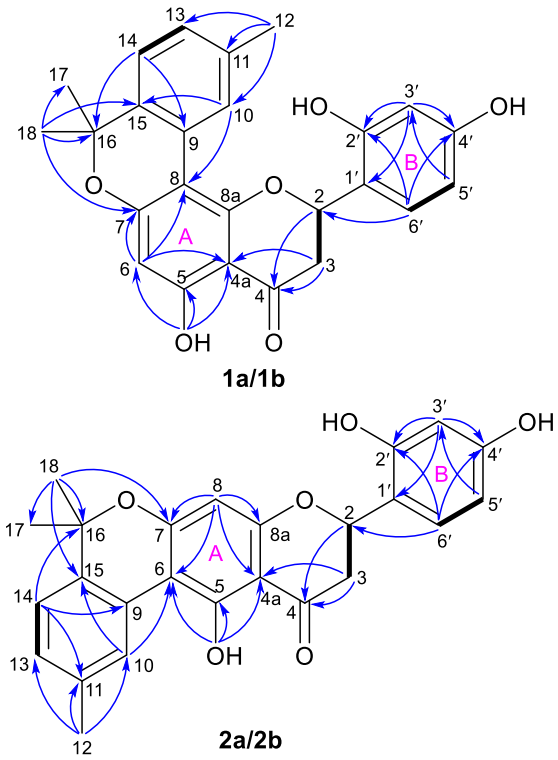

Figure 3. 2D NMR correlations for compounds 1a/1b and 2a/2b.

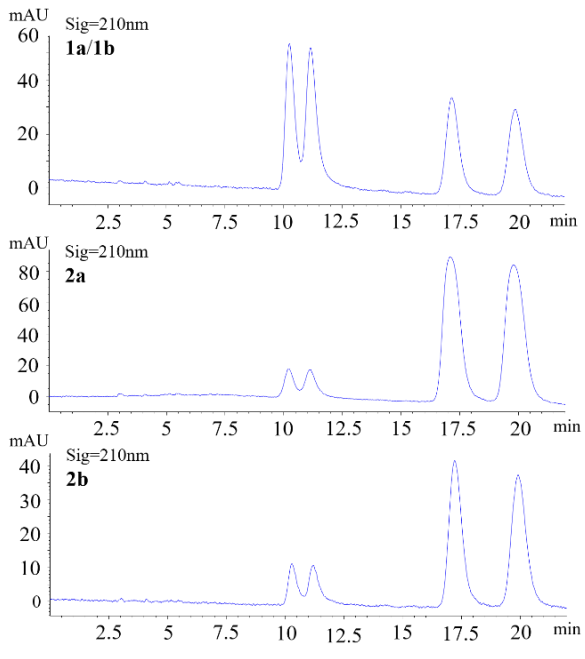

Figure 4. Comparison of chiral HPLC chromatograms for 1a/1b, 2a and 2b.

It was confusing that the two pairs of enantiomers **1a**/**1b** and **2a**/**2b** were well separated on the chiral column (Figure 2) but their NMR spectra after chiral HPLC purification still showed signals of a mixture, which was comparable to the original sample. This phenomenon implied a possible transformation between the two pairs of molecules, and their nearly flat ECD curves (Supplemental Figure S21) and small or close-to-zero $[\alpha]_D$ values (Supplemental Figures S22–S25) further suggested the likely presence of enantiomerization during their mutual isomerization process, which resulted in an equilibration among them. Therefore, the structure characterization at this stage was continued via interpretation of the spectroscopic data of the mixture.

Analyses of the NMR data (in CD_3OD, Table 1) for the minor components **1a**/**1b** revealed the presence of a carbonyl (δ_C 199.6), an oxygenated methine [δ_C 76.5; δ_H 5.82 (dd, J = 13.5, 2.8 Hz)] and a methylene [δ_C 42.5; δ_H 3.26 (dd, J = 17.0, 13.5 Hz), 2.85 (dd, J = 17.0, 2.8 Hz)] groups, which were characteristic for the C-4, CH-2 and CH_2-3 of a flavanone like sanggenol L (Figure 1) [22]. More signals for a 1,2,4-trisubstituted benzene at δ_H 7.39 (d, J = 8.5 Hz), 6.40 (dd, J = 8.5, 2.5 Hz) and 6.39 (d, J = 2.5 Hz), and at δ_C 160.1, 157.3, 128.9, 117.3, 107.7 and 103.5, as well as for a penta-substituted benzene at δ_H 6.07 (s) and at δ_C 164.3, 164.0, 162.6, 105.3, 104.5 and 99.4, were also observed, and the two fragments corresponded to the B and A rings of the flavanone core, respectively, as in sanggenol L [22]. The major difference between the two analogues was attributed to that the monoterpenyl forming a pyran unit with ring A in sanggenol L rearranged to form a benzopyran unit with ring A in **1a**/**1b**, which was evidenced by the resonances for a 1,3,4-trisubstituted aromatic fragment at δ_H 8.28 (d, J = 1.1 Hz), δ_H 7.14 (d, J = 7.9 Hz), δ_H 7.02 (dd, J = 7.9, 1.1 Hz), and at δ_C 138.0, 136.6, 128.5, 128.0, 127.5, 123.4. The connection of the monoterpenyl unit to ring A was confirmed by the HMBC signal from H-10 to C-8 and the long-range J^4 correlation from H_3-18 to C-7. Also, the HMBC correlations (in CD_3COCD_3) from 5-OH to C-4a, C-5 and C-6 (a methine carbon) further corroborated that the monoterpenyl substitution on ring A was at C-8 instead of C-6, otherwise, 5-OH would have shown HMBC correlations to all quaternary carbons. A comprehensive inspection of the full 2D NMR data (Figure 3) corroborated the constitution structure of **1a**/**1b** as shown, and other important HMBC signals included those from H-2 and H_2-3 to C-4, H_3-12 to C-10, C-11 and C-13, H_3-18 to C-15, C-16 and C-17, H-6′ to C-2. The planar structure of **1a**/**1b** was thus established.

With the structure of **1a**/**1b** in hand, the structure characterization for **2a**/**2b** then became self-evident. By careful analyses of the NMR data for the two pair of co-isolates (Table 1), it was obvious that they incorporated the same flavanone scaffold and only differed from each other at the substitution location of the monoterpenyl unit, which was connected to C-6 rather than C-8 in **2a**/**2b** as supported by the HMBC correlations (in CD_3COCD_3) from 5-OH to C-4a, C-5 and C-6 (all quaternary carbons, Figure 3). This assignment was also confirmed by the chemical shift difference for 5-OH in **1a**/**1b** (δ_H 12.51) and **2a**/**2b** (δ_H 13.73), which was consistent with the empirical rule that 5-OH in 6-prenylflavonoids is more deshielded than its counterpart in 8-prenylflavonoids [23].

To further investigate the possible transformation of theses interesting molecules, all the samples of **1a**/**1b**, **2a** and **2b** were further analyzed by the same chiral column after their spectroscopic measurements were completed. As shown in Figure 4, the chiral HPLC chromatograms of them all displayed four peaks like the original mixture, which firmly supported the aforementioned conclusion that the four isomers would undergo a mutual transformation. In order to obtain good NMR data, compounds **1a** and **1b** (both with limited sample amount) was mixed again after we knew their enantiomeric relationship and measured their other spectroscopic data, so the chiral HPLC analysis here was performed on their mixture. We then proposed a plausible mechanism for this chemical transformation among **1a**, **1b**, **2a** and **2b** as shown in Scheme 1. On reviewing the literature, the isomerization at C-2 was once described for sanggenol L and related analogues [23], but the regio-isomerization between C-6 and C-8 substitution had not been reported previously. We speculate that the aromatic monoterpenyl group has extended the conjugation system and could facilitate the formation of the intermediates by stabilizing them.

Hyperglycemia is a major symptom of type 2 diabetes mellitus, and thus controlling hyperglycemia with α-glucosidase inhibitors has been demonstrated to be a strategy for the glycemic modulation and prevention of type 2 diabetes [24]. Following our previous work on the exploration of natural α-glucosidase inhibitors from plant resources [18-20, 25] the anti-hyperglycemic effect of **1a**/**1b**, **2a** and **2b** was evaluated by testing the *in vitro* α-glucosidase inhibitory activity of them, with IC_{50} values of 4.05 ± 0.65, 3.06 ± 0.42 and 6.69 ± 0.51 μM, respectively. These flavanone-monoterpene hybrids showed much better activity than the positive control acarbose which had an IC_{50} of 359.10 ± 2.39 μM.

Table 1. NMR data for compounds 1a/1b and 2a/2b

No.	**1a/1b**[a]		**1a/1b**[b]		**2a/2b**[a]		**2a/2b**[b]	
	δ_C	δ_H (*J* in Hz)	δ_C	δ_H (J in Hz)			δ_C	δ_H (*J* in Hz)
2	76.5	5.82, dd (13.5, 2.8)	76.0	5.91, m	76.0	5.69, dd (13.3, 2.9)	75.4	5.79, m
3	42.5	3.26, dd (17.0, 13.5) 2.85, dd (17.0, 2.8)	42.1	3.30, m	43.3	3.20, dd (17.1, 13.3) 2.79, dd (17.1, 2.9)	42.7	3.30, m
4	199.6		199.1		199.6		199.1	
4a	104.5		104.9		104.5		104.3	
5	164.3		164.4		164.3		162.5	
6	99.4	6.07, s	99.0	6.07, s	105.3		104.8	
7	164.0		163.3		164.0		163.8	
8	105.3		104.5		98.4	6.09, s	97.9	6.08, s
8a	162.6		161.3		162.6		163.2	
1'	117.3		116.9		117.6		117.1	
2'	157.3		156.7		156.9		156.4	
3'	103.5	6.39, d (2.5)	103.5	6.57, d (2.3)	103.4	6.34, d (2.3)	103.5	6.49, d (2.3)
4'	160.1		159.9		159.9		159.6	
5'	107.7	6.40, dd (8.5, 2.5)	107.8	6.49 dd (8.4, 2.3)	107.8	6.35, dd (8.2, 2.3)	108.0	6.45, dd (8.4, 2.3)
6'	128.9	7.39, d (8.5)	129.0	7.49, d (8.4)	129.0	7.26, d (8.2)	129.2	7.35, d (8.4)
9	127.5		127.2		128.0		127.8	
10	128.0	8.28, d (1.1)	127.8	8.34, brs	127.6	8.35, d (1.6)	127.2	8.37, d (1.7)
11	138.0		137.5		138.1		137.7	
12	21.4	2.22, s	21.4	2.22, s	21.6	2.37, s	21.6	2.36, s
13	128.5	7.02, dd (7.9, 1.1)	128.3	7.04, dd (7.8, 1.6)	128.6	7.08, dd (7.9, 1.6)	128.5	7.11, dd (7.9, 1.7)
14	123.4	7.14, d (7.9)	123.4	7.19, d (7.8)	123.5	7.18, d (7.9)	123.5	7.23, d (7.9)
15	136.6		136.2		136.4		136.0	
16	80.1		79.7		80.2		79.8	
17	27.8	1.56[c], s	27.7	1.58[d], s	27.85[e]	1.59[f], s	27.8	1.61[g], s
18	27.8	1.61[c], s	27.7	1.61[d], s	27.89[e]	1.60[f], s	27.8	1.62[g], s
5-OH				12.50				13.73

Note: [a] in CD_3OD; [b] in CD_3COCD_3; [c–g] Interchangeable assignment

Supplementary materials

Supplementary Figures S1–S25 are available online at *TMR Modern Herbal Medicine*. Raw MS, NMR, ECD and $[\alpha]_D$ spectra can be obtained by contacting the corresponding author.

References

1. Zhang XQ, Wu ZY. Flora of China. Beijing: Science Press, 1998. (Chinese)
2. Ibrahim K, Zhu W, Li KK, et al. Polyphenols of mulberry fruits as multifaceted compounds, Compositions, metabolism, health benefits, and stability – A structural review. *J. Funct. Foods*. 2018;40:28–43. https://doi.org/10.1016/j.jff.2017.10.041
3. Yuan QX, Zhao LY. The Mulberry (*Morus alba* L.) Fruit- A Review of Characteristic Components and Health Benefits. *J. Agric. Food Chem*. 2017;65:10383–10394. https://doi.org/10.1021/acs.jafc.7b03614
4. Chen C, Razali UHM, Saikim FH, et al. *Morus alba* L. Plant: Bioactive Compounds and Potential as a Functional Food Ingredient. *Foods*. 2021;10:689. https://doi.org/10.3390/foods10030689
5. Chan EWC, Lye PY, Wong SK. Phytochemistry, pharmacology, and clinical trials of *Morus alba*. *Chin. J. Nat. Med*. 2016;14(1):17–30. https://doi.org/10.3724/SP.J.1009.2016.00017
6. Chinese Pharmacopoeia Commission. Pharmacopoeia of the People's Republic of China (part one). Beijing: China Medical Science Press, 2015. (Chinese)
7. Deshpande VH, Parthasarathy PC, Venkataramn K. Four analogues of artocarpin and cyclotocarpin from *Morus alba*. *Tetrahedron Lett*. 1968;9(14):1715–19. https://doi.org/10.1016/S0040-4039(01)99035-5
8. Ha MT, Shrestha S, Tran TH, et al. Inhibition of PTP1B by farnesylated 2-arylbenzofurans isolated from *Morus alba* root bark, unraveling the mechanism of inhibition based on *in vitro* and *in silico* studies. *Arch. Pharm. Res*. 2020;43:961–975. https://doi.org/10.1007/s12272-020-01269-4
9. Manh TH, Su HS, Tien DN, et al. Chalcone derivatives from the root bark of *Morus alba* L. act as inhibitors of PTP1B and *α*-glucosidase. *Phytochemistry*. 2018;155:114–125. https://doi.org/10.1016/j.phytochem.2018.08.001
10. Chang YS, Jin HG, Hwan L, et al. Phytochemical Constituents of the Root Bark from *Morus alba* and Their Il-6 Inhibitory Activity. *Nat. Prod. Sci*. 2019;25(3):268–274. https://doi.org/10.20307/nps.2019.25.3.268
11. Ko WM, Liu ZM, Kim KW, et al. Kuwanon T and Sanggenon a Isolated from *Morus alba* Exert Anti-Inflammatory Effects by Regulating NF-κB and HO-1/Nrf2 Signaling Pathways in BV2 and RAW264.7 Cells. *Molecules* 2021;26(24):7642. https://doi.org/10.3390/molecules26247642
12. Marie C, Alice S, Sherif TSH, et al. Multiple In vitro biological effects of phenolic compounds from *Morus alba* root bark. *J. Ethnopharmacol*. 2020;248:112296. https://doi.org/10.1016/j.jep.2019.112296
13. Wang JX, Liu XQ, Zheng H, et al. Morusin induces apoptosis and autophagy via JNK, ERK and PI3K/Akt signaling in human lung carcinoma cells. *Chem. Biolo. Interact*. 2020;331:109279. https://doi.org/10.1016/j.cbi.2020.109279
14. Min TR, Park HJ, Park MN, et al. The Root Bark of *Morus alba* L. Suppressed the Migration of Human Non-Small-Cell Lung Cancer Cells through Inhibition of Epithelial–Mesenchymal Transition Mediated by STAT3 and Src. *Int. J. Mol. Sci*. 2019;20(9):2244. https://doi.org/10.3390/ijms20092244
15. Xia CL, Tang GH, Guo YQ, et al. Mulberry Diels-Alder-type adducts from *Morus alba* as multi-targeted agents for Alzheimer's disease. *Phytochemistry*. 2019;157:82–91. https://doi.org/10.1016/j.phytochem.2018.10.028
16. Paudel P, Park SE, Seong SH, et al. Novel Diels–Alder Type Adducts from *Morus alba* Root Bark Targeting Human Monoamine Oxidase and Dopaminergic Receptors for the Management of Neurodegenerative Diseases. *Int. J. Mol. Sci*. 2019;20(24):6232. https://doi.org/10.3390/ijms20246232
17. Shahnaz A, Farak A, Sheikh RA, et al. Phytochemistry and Pharmacological Properties of *Morus alba* Linn. with Reference to its SARS-CoV-2 Inhibiting Potential. *Asian J. Chem*. 2022;34(8):1983−1992. https://doi.org/10.14233/ajchem.2022.23891
18. Yu SJ, Yu JH, Yu ZP, et al. Bioactive terpenoid constituents from *Eclipta prostrata*. *Phytochemistry*. 2020;170:112192. https://doi.org/10.1016/j.phytochem.2019.112192
19. Song XQ, Yu JH, Sun J, et al. Bioactive sesquiterpenoids from the flower buds of *Tussilago farfara*. *Bioorg. Chem*. 2021;107:104632.

https://doi.org/10.1016/j.bioorg.2021.104632
20. Xu DF, Miao L, Wang YY, et al. Chemical constituents from *Tinospora sagittata* and their biological activities. *Fitoterapia.* 2021;153:104963. https://doi.org/10.1016/j.ftote.2021.104963
21. Song XQ, Sun J, Yu JH, et al. Prenylated indole alkaloids and lignans from the flower buds of *Tussilago farfara*. *Fitoterapia.* 2020;146:104729. https://doi.org/10.1016/j.fitote.2020.104729
22. Jung JW, Ko WM, Park JH, et al. Isoprenylated flavonoids from the root bark of *Morus alba* and their hepatoprotective and neuroprotective activities. *Arch. Pharm. Res*. 2015;38(11):2066-2075. https://doi.org/10.1007/s12272-015-0613-8
23. Shi YQ, Fukai T, Sakagami H, et al. Cytotoxic Flavonoids with Isoprenoid Groups from *Morus mongolica*. *J. Nat. Prod*. 2001;64:181–188. https://doi.org/10.1021/np000317c
24. Ros JL, Francini F, Schinella GR. Natural Products for the Treatment of Type 2 Diabetes Mellitus. *Planta Med*. 2015;81:975–994. http://dx.doi.org/10.1055/s-0035-1546131
25. Zhang JS, Xu DF, Wang YY, et al. Clerodane furanoditerpenoids from the stems of *Tinospora sinensis*. *Arch. Pharm. Res*. 2022;45:328–339. https://doi.org/10.1007/s12272-022-01383-5